MATHEWS JOURNAL OF CANCER SCIENCE

MATHEWS Open Access Journals

Research Article

Vol No: 05, Issue: 01

Received Date: Feb 02, 2020

Published Date: May 29, 2020

C-M Charlie Ma*

Xiaoming Chen

Alain Tafo

Dusica Cvetkovic

Lili Chen

Department of Radiation Oncology, FoxChase Cancer Center, Philadelphia, PA19111, USA

Corresponding Author:

C-M Charlie Ma*

Radiation Oncology Department, FoxChase Cancer Center, 333 Cottman Avenue, Philadelphia, PA19111, USA.

E-mail: Charlie.Ma@fccc.edu

The Nonthermal Therapeutic Effect of Pulsed Focused Ultrasound

ABSTRACT

Purpose: Many studies have been carried out on the use of high-intensity focused ultrasound (HIFU) for tissue ablation and enhancement of drug delivery for various therapies. This work aims to investigate the nonthermal therapeutic effect of pulsed focused ultrasound (pFUS) for cancer treatment.

Method: This study used a MR-guided HIFU system (InSightecExAblate 2000), which is integrated with a 1.5T GE MR scanner, for *in vitro* and *in vivo* experiments. Ultrasound parameters derived from previous studies were used to perform nonthermal sonications, keeping tissue temperatures below 42°C as measured in real time by MR thermometry. MCF-7, LNCaP and PC3 cells were used in the in vitro cell survival experiments and implanted in nude mice for in vivo studies. The tumor cells and the tumor-bearing mice were treated with pFUS (5, 6 and 25W acoustic power; 1MHz frequency; 10% and 50% duty cycle; 60 sec duration). Implanted tumors were treated with 4-6 sonications guided by MR imaging. The clonogenic assay and trypan blue dye analysis were performed for treated tumor cells. High-resolution (0.2mm) MRI was used weekly to measure tumor growth for both treated animals and the control group.

Results: The *in vitro* experimental results showed significa t nonthermal cell damage by pFUS exposures. For LNCaP cells, 10.6 and 33.6% cell deaths were observed for 6 and 10W acoustic power, respectively. Significa t tumor growth delay was observed in the pFUS-treated tumor-bearing mice. The mean tumor volume for the pFUS-treated mice was 20-30% smaller than that of the control mice one week after the pFUS treatment depending on the acoustic powers and duty cycles used.

Conclusions: Our *in vitro* and In vivo experimental results have confi med the nonthermal therapeutic effect of pFUS. More systematic studies are needed to derive optimal ultrasound parameters and fractionation schemes to maximize the therapeutic potential of pFUS. Further investigations are warranted to understand the mechanism of pFUS-induced nonthermal cell damage.

Keywords: High-intensity focused ultrasound (HIFU); Pulsed focused ultrasound (pFUS); MR guidance; Thermal ablation; Nonthermal effect; Therapeutic effect; Breast cancer; Prostate cancer

INTRODUCTION

High-intensity focused ultrasound (HIFU) has many medical applications including thermal tissue ablation for the treatment of uterine fib oids and

DOI: https://doi.org/10.30654/MJCS.10025

various solid cancers [1-8]. Recently, it has been demonstrated that pulsed HIFU, or pulsed focused ultrasound (pFUS) may be used to alter tissue properties such as the vascular or cell membrane permeability for the enhancement of drug delivery for various therapies such as gene therapy and chemotherapy [9-18]. The nonthermal (<42°C) effects of pFUS have shown similar cell damage characteristics of high linear energy transfer (LET) radiation that is less affected by the cell radiation resistance and local biochemical environment [19-23].

In our previous studies, we have developed MR-guided HIFU (MRgHIFU) therapy techniques using a clinical HIFU treatment device (InSightecExAblate 2000) integrated with a 1.5T MR scanner (Signa Excite HD, GE Healthcare, Milwaukee, WI, USA) for MR image-guidance during treatment. We have performed *in vitro* cell experiments and *in vivo* studies using a small animal model (nude mouse) to investigate the enhancement of drug delivery for chemotherapy and gene therapy in prostate tumors grown in nude mice orthotopically [14-16]. A preliminary *in vivo* study on the nonthermal effect of pFUS was carried out using one pFUS parameter setting and one human tumor cell line (LNCaP) implanted in nude mice [23].

This study is aimed to further investigate the nonthermal effect of pFUS and its therapeutic potential for cancer treatment. Exploratory in vitro cell experiments and *in vivo* animal treatments with implanted tumors have been carried out using a clinical MR-guided HIFU system. The MRgHIFU system and the pFUS treatment procedures will be described in detail. The therapeutic effect of pFUS has been quantified with clonogenic assay and trypan blue dye exclusion in an *in vitro* cell survival study. High-resolution 3D MR imaging has been used to evaluate the tumor growth delay after pFUS treatment of tumor-bearing mice *in vivo*. Three human tumor cell lines have been investigated including breast cancer (MCF-7) and prostate cancer (LNCaP, PC3) cell lines and pFUS treatment was performed with various ultrasound parameter settings. The pFUS results have been compared with those of radiation therapy using the same animal model to provide useful information for the design of future studies on the dose-response relationship and fractionation effects of pFUS for cancer therapy.

MATERIALS AND METHODS

Experimental Setup

A clinical MRgHIFU system (ExAblate 2000, InSightec-Tx-Sonics, Haifa, Israel) integrated with a 1.5T GE MR scanner was used for the pFUS sonications (**Figure 1**). This MRgHIFU system has been approved by the FDA for the treatment of uterine fib oids and bone palliation [14]. We have performed clinical investigations of MRgHIFU for prostate and breast cancer ablation under local IRB approval [17,23]. Routine quality assurance (QA) and quality control (QC) programs have been developed for the clinical MRgHIFU treatment unit to ensure the focal spot, transducer output and electronic motion control before pFUS treatments [14,24].

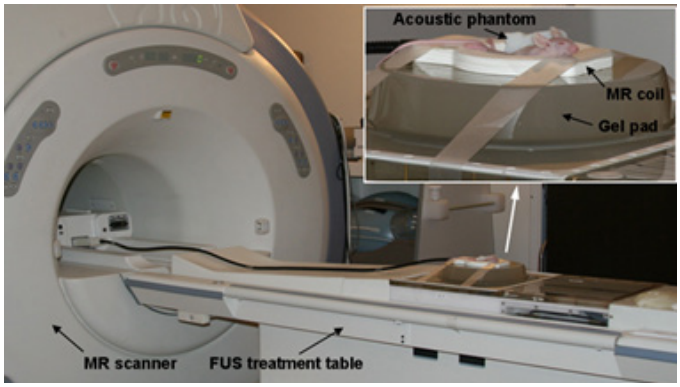

Figure 1: The GE 1.5T MR scanner and InSightecMRgHIFU system used for this study. The insert shows the animal setup for the pFU experiment.

In vitro Cell Survival Study

For this study, human breast cancer (MCF-7) and prostate cancer (LNCaP and PC3) cells were obtained from the American Type Culture Collection and cultured in Dulbecco's modified Eagle's medium (DMEM)-F12 medium, containing 10% fetal bovine serum (FBS), 1% L-glutamine, and 1% penicillin-streptomycin. Cells were maintained at 37°C and in a humidified atmosphere of 5% CO_2. Only LNCaP and PC3 cells were used for the *in vitro* experiment. The cell suspension was contained in a 2-mm thin plastic vessel and inserted in an ultrasound gel phantom with the ultrasound beam focused on the center of the vessel. Cells were exposed to pFUS (1MHz; 6W and 10 W acoustic power; 5Hz frequency; 50% duty cycle: 0.1s power on, 0.1s power off) for 60 seconds. Cell viability was assessed by trypan blue dye exclusion and clonogenic assay. The percentage of dead cells was measured by trypan blue dye exclusion at 24h after pFUS. Immediately after pFUS, cells were counted, and known numbers of cells were plated into 100-mm dishes. The plates were incubated for 14 days and stained with 0.25% methylene blue. The colonies were counted.

In vivo Tumor Model

It is important to use a good in vivo tumor model that is well confined locally and less likely to metastasize to other organs [14,16,23,25]. Both female and male nude mice (six weeks old) were purchased from Harlan (Indianapolis, IN). Our animal studies were performed according to procedures approved by the institutional animal care and use committee (IACUC).

Aseptic techniques were used for injection and implantation of breast MCF-7 cells subcutaneously in the flanksof female mice and prostate LNCaP cells orthotopically in the prostates of male mice under anesthesia. Tumors were allowed to grow and then randomized into control and treatment groups.

MR Imaging

In our study, MR imaging played an essential role in the entire treatment process. It was used for the mouse setup, focal spot check and target delineation before treatment, and target localization, temperature monitoring and treatment assessment during treatment. The tumor volume was measured by MR imaging both before and after the pFUS treatment following a standard imaging protocol established in previous studies [14,16]. T2-weighted MR images were acquired using fast-recovery fast-spin-echo (FRFSE) sequence, TR/TE = 2200/85 ms, NEX = 3, matrix = 288 × 288, FOV = 7 × 7cm^2 (resolution = 0.243 × 0.243mm^2), and slice thickness = 2mm for coronal and = 1mm for axial scans, respectively.

Pulsed Focused Ultrasound Treatment

Pulsed focused ultrasound treatment was performed using a previously described method with minor modific tions [14]. Tumor-bearing mice were randomized for treatment. Mice were anesthetized by the intraperitoneal injection of a mixture of Ketamine (60 mg/kg) and Ace-promazine (2.5 mg/kg). The total anesthesia time was about 1 hour which is suffici t for pre-treatment MR imaging, treatment planning, and pFUS sonications. Figure 1 shows the treatment setup. A gel pad was placed on the HIFU table in line with the transducer with degassed water in the interface between the table and the gel pad. The mouse was placed in the hole (5cm × 5cm × 1cm) of gel pad with degassed water. A 3-inch surface coil was placed around the mouse for MR imaging. A vendor-supplied acoustic phantom was also placed in the MR coil to verify the focal spot. To protect the mouse from hypothermia, a surgical glove filled with warm water was used to cover the animal. Both coronal and axial MR images were used for tumor volume delineation and a sonication plan was generated based on the target volume and shape. High-spatial-resolution (0.8 × 1.7 × 2.0 mm) proton resonance frequency shift MR thermometry was performed to verify the effective ultrasound focal spot prior to sonication usinga small acoustic phantom beside the animal [3,23,24]. The treatment parameters were derived from acoustic phantom measurements as described by Chen L, et al. [14]. Mice were treated with 1 MHz ultrasound, 5 and 25W acoustic power, 10 and 50% duty cycle and 60 second duration per sonication. The estimated time averaged acoustic focal intensity was about 1100 W/cm^{2}for 25 W acoustic power according to the vendor's manual. The focal volume was cigar-shaped with a diameter of 3.8 mm and a length of 10.3 mm according to the ultrasound parameters used. The tissue temperature was monitored in real time by MR thermometry to ensure it was less than 42^{o}C.

Radiation Treatment

The radiation treatment has been reported previously (15,23) and the results are compared in this study with the new pFUS results. The purpose of this side-by-side comparison was to quantify the therapeutic effects of pFUS and RT for the same tumor model to facilitate the design of future pFUS studies on desirable dose and fractionation, which is well understood in RT. For completeness, the radiation procedure is briefly described here. The mouse was restrained under general anesthesia in the supine position with tape in a jig and treated with 6 MV photon beams on a Siemens Artiste linear accelerator (Siemens Medical Solutions, Concord, CA). A 1.5 cm tissue-equivalent bolus was used and the source-to-surface distance was kept at 100cm. A collimator was used to treat the prostate while protecting the rest of the body. A single dose of 2 Gy was delivered to the tumor at a dose rate of 300 MU per minute.

Tumor Growth Measurement

After tumor implantation, mice were scanned weekly for tumor growth monitoring using a 1.5T GE MR scanner and the imaging protocol described earlier. The tumor was contoured on the axial MR images with a resolution of 0.243 × 0.243 mm^2. The tumor area was calculated by summing up the number of pixels within the tumor contour. The total tumor volume was calculated by adding up the tumor area on each MR image and multiplying the slice thickness (= 1mm). This measurement technique was compared with caliper measurements and validated using a 7T small bore animal MR scanner (Bruker Biospin MRI, Billerica, MA).

Data Analysis and Statistics

Statistical analysis was performed for the measured tumor cells *in vitro* and tumor volumes *in vivo*. The mean and standard deviation of the mean (SEM) were calculated and the results were expressed as mean ± SEM. To determine if there was a significa t difference among different groups, a Student's t-test was used and a p-value, $p \leq 0.05$, was considered to be statistically significa t.

DOI: https://doi.org/10.30654/MJCS.10025

RESULTS

In vitro Cell Survival Studies

Nonthermal cell damage by pFUS exposure was observed for both LNCaP and PC3 cells based on trypan blue dye analysis. The pFUS exposures were given either at 6 W or 10 W at 1MHz, 5Hz frequency,50% duty cycle and 60 seconds duration. The maximum temperature elevation was below 5º Cas measured MR thermometry within the focal zone. At 6W acoustic powers, the cell-death rate due to pFUS was 10.6+1.7% and at 10W it was 34.6+1.9% for the LNCaP cells compared to the control cell. For PC3 cells, the cell-death rate was 9.7+0.9% at 6W and 27.0+1.6% at 10 W, respectively. The clonogenic assay results were similar to the trypan blue dye analysis (LNCaP: 14.4+2.5% at 6 W and 31.3+2.7% at 10 W; PC3: 11.2+2.9% at 6 W and 24.6+3.5% at 10 W).

Tumor Volume Measurement

Three measurement procedures have been investigated in this work to determine the tumor volume accurately. The MR imaging procedures were similar, either performed on a 1.5T clinical MR scanner, which is conveniently located in our department and integrated with the clinical HIFU treatment system, or on a 7T Bruker small bore animal MR scanner, which is located in a separate laboratory. **Figure 2(a)** shows tumor volumes measured by MRI on the 1.5T MR scanner and the 7T Bruker MR scanner for 5 subcutaneous breast tumors. The average difference in volume was 1.5% ± 0.6% between the two scanners. The Vernier caliper measurement is the easiest method if the tumor is directly under the skin and the measurement can be performed without anesthesia. However, the caliper measurement results can be quite uncertain as compared to the tumor volumes determined by MR imaging. **Figure 2(b)** shows tumor volumes measured by a Vernier caliper and MRI on the 1.5T MR scanner for 9 mice. Large (> 30%) differences were found, depending on the tumor size, between the volumes determined by the caliper measurement and those measured by MRI. For better consistency between pretreatment imaging for treatment planning and post-treatment tumor-volume assessment, and easy accessibility, all tumor volume measurements have been performed on the 1.5T MR scanner in our department for this study.

Skin Response to pFUS

Normal tissue toxicity has been a concern for pFUS even though the elevation of tissue temperature has been kept low to avoid thermal damage to normal structures. **Figure 3** shows intact mouse skin before and one week after the pFUS treatment. The mouse was treated on the MRgHIFU system with ultrasound parameters: 1MHz, 25W (10MPa) acoustic power, 10%duty cycle and 60s duration per sonication. Under the same conditions, a temperature elevation of <5ºC was confi med in a tissue-mimicking phantom and in targeted tumor tissues in mice as measured by MR thermometry while the mouse temperature measured by an anal thermometer under anesthesia before and after the imaging/treatment procedure was 37ºC and 30ºC, respectively. It was intended to keep the tissue temperature <42ºC so that any observed therapeutic effect would be predominantly nonthermal.

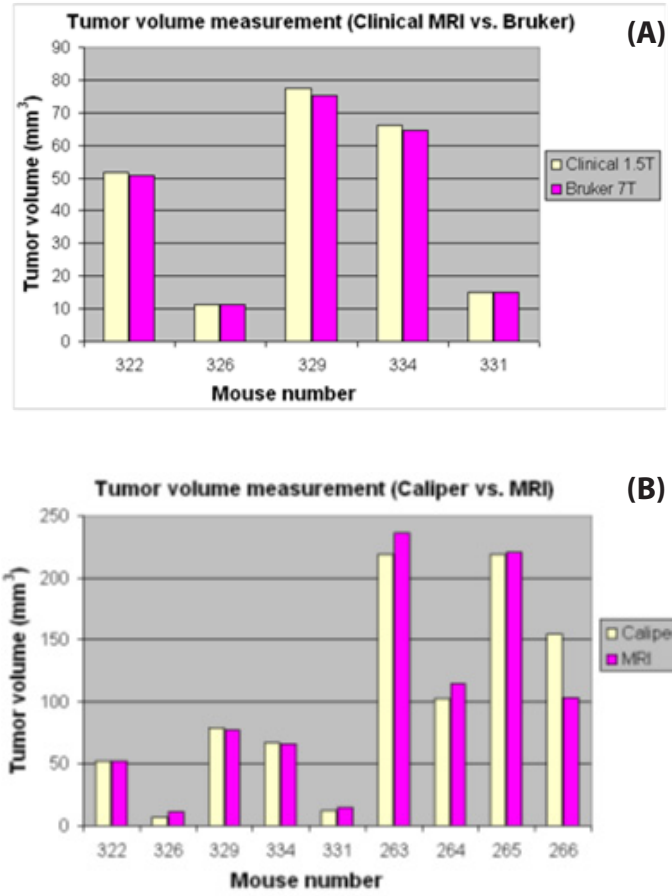

Figure 2: Tumor volumes measured by MRI on a clinical 1.5T GE MR scanner and a 7T Bruker animal MR scanner (a) and by caliper and MRI on the 1.5T GE scanner. Mice were implanted with breast (MCF-7) cells subcutaneously.

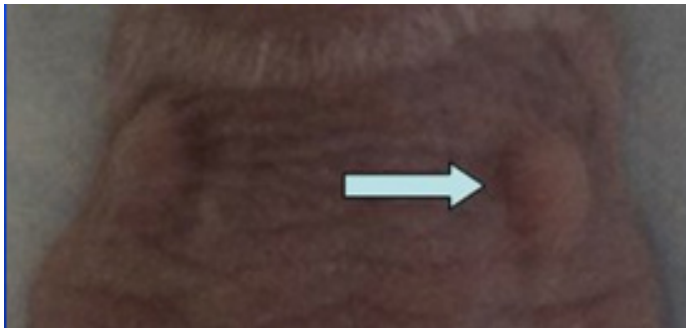

(a)

DOI: https://doi.org/10.30654/MJCS.10025

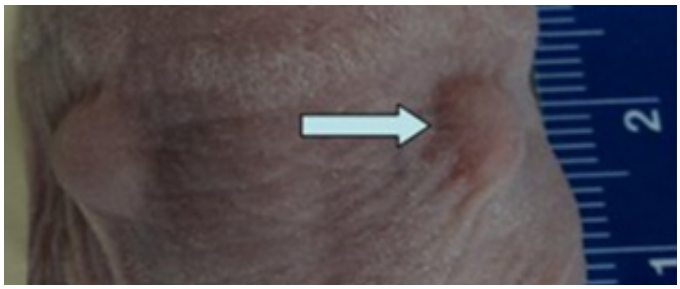

(b)

Figure 3: Mouse skin before pFUStreatment (a) and 1 week after pFUS treatment (b).Arrows point to the tumor treated with pFUS.

Since the tumor dimension (~ 5mm) was much smaller than the length of the ultrasound focal volume (10.3mm), the mouse skin was certainly within the focal volume and received similar pFUS exposures as the tumor cells immediately adjacent to it. However, no skin damage was observed after pFUS treatment as shown in Fig. 3. For mice implanted with prostate cancer cells orthotopically, the pFUS treatment target was surrounded by critical organs such as the rectum, bladder and bowel, which at least were partially, exposed to similar high-intensity ultrasound pulses as the treatment target. No skin damage was observed for these mice up to 2 months after the pFUS treatment and no tissue damage in any organs around the treatment target in sacrifi ed animals.

Tumor Response to pFUS

In vivo animal studies have been carried out on the nonthermal effect of pFUS on two human tumor cell lines (MCF-7 and LNCaP) with two pFUS parameter settings (5W with a 50% duty cycle and 25W with a 10% duty cycle). It was expected that the two pFUS power levels would deliver similar ultrasound energy for the same 60s sonication but at different intensity levels that would lead to different therapeutic effects while keeping the tissue temperature elevation below 5°C. **Figure 4** shows the mean tumor volumes measured weekly for the control mice and pFUS treated mice implanted with breast (MCF-7) cancer cells. The ultrasound parameters were 1MHz, 25W (10MPa) acoustic power, 10%duty cycle and 60s exposure duration. This is the lowest duty cycle available on our clinical MRgHIFU system. A continuous and slightly decelerated growth was observed for the control mice. As tumors grew some tumors developed separate lobes and necrotic zones appeared inside the tumors. For mice exposed to pFUS, significa t tumor growth delay was observed for all mice at different time points after the pFUS treatment (p values less than 5%).

Since our previous investigation has explored the pFUS setting at 25W and 10% duty cycle for LNCaP tumor cells we further investigated a lower pFUS power setting. **Figure 5** shows the mean tumor volumes measured weekly for the control mice and pFUS treated mice implanted with prostate (LNCaP) tumor cells, normalized to the volume on the day of treatment. The ultrasound parameters were 1MHz, 5W acoustic power, 50% duty cycle and 60s duration of sonication. A continuous and slight accelerated growth was observed for the control mice. For mice exposed to pFUS, significa t tumor growth delay was also observed for all mice compared to the control group ($p = 0.19$ for one week after treatment). For pFUS treated mice, the relative mean tumor volume was 1.073 one week after treatment, 1.76 two weeks after treatment and 2.54 three weeks after treatment while it was 1.037, 1.94 and 2.67 for the control mice, respectively. The tumor growth delay at one week after pFUS treatment was significa t ($p = 0.019$). The mean tumor volume only increased slightly one week after the pFUS treatment.

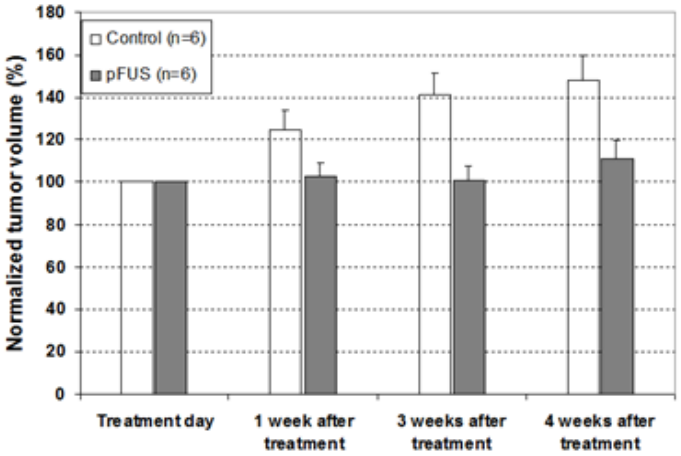

Figure 4: Mean tumor volumes for pFUS treated mice implanted with breast (MCF-7) cancer cells (n = 6) and control mice (n = 6).

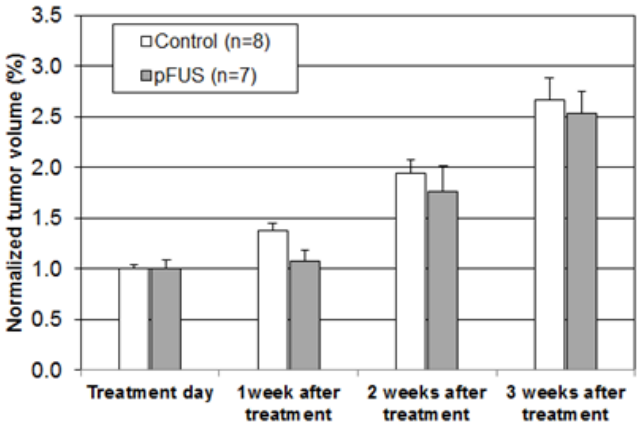

Figure 5: Mean tumor volumes for pFUS treated mice implanted with prostate (LNCaP) cancer cells (n=7) and control mice (n=8). The ultrasound parameters: 5W acoustic power with50%duty cycle and 60s duration.

To further investigate the tumor growth delay due to pFUS, tumor-bearing mice were treated twice with pFUS at the same power setting at one week interval. The mean tumor

DOI: https://doi.org/10.30654/MJCS.10025

volumes of the control mice and pFUS-treated mice implanted with LNCaP tumor cells are shown in **figu e 6**. The pFUS parameters for each pFUS treatment were 1MHz, 5W acoustic power, 50% duty cycle and 60s duration of sonication. Similar tumor growth delay was obtained in both pFUS treatments at one week after the pFUS treatment (i.e., an accumulative 40% tumor growth delay by both pFUS treatments). No skin damage was observed for mice treated twice with pFUS at this power setting, indicating that it is possible to repeat the pFUS treatment on the same animals. This is important if pFUS will be used for fractionated therapy applications.

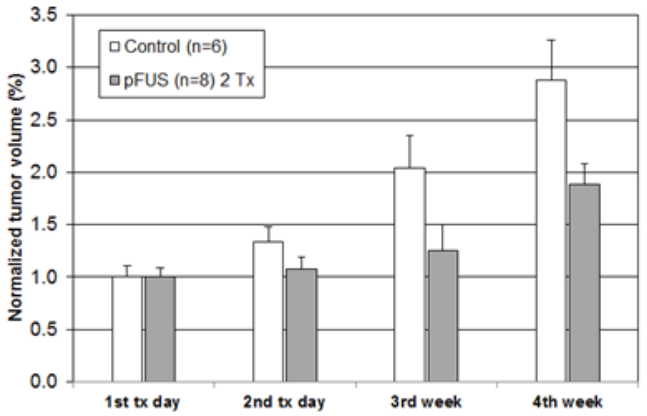

Figure 6: Mean tumor volumes for pFUS treated mice implanted with prostate (LNCaP) cancer cells (n = 8) and control mice (n = 6). The mice received two pFUS treatments at a1-week interval (US parameters: 5W acoustic power, 50%duty cycle and 60s duration).

Tumor growth delay by pFUS treatment has been compared with that by radiation therapy (RT) to quantify its therapeutic potential. **Figure 7** shows the ratios of the tumor volumes treated by pFUS and RT to the corresponding tumor volumes of the control mice at different time points post treatment, normalized to the values on the day of treatment. The mice were implanted with LNCaP tumor cells and treated with pFUS with 5 W acoustic power and 50% duty cycle or 25 W acoustic power and 10% duty cycle, and with RT for 2Gy, respectively.

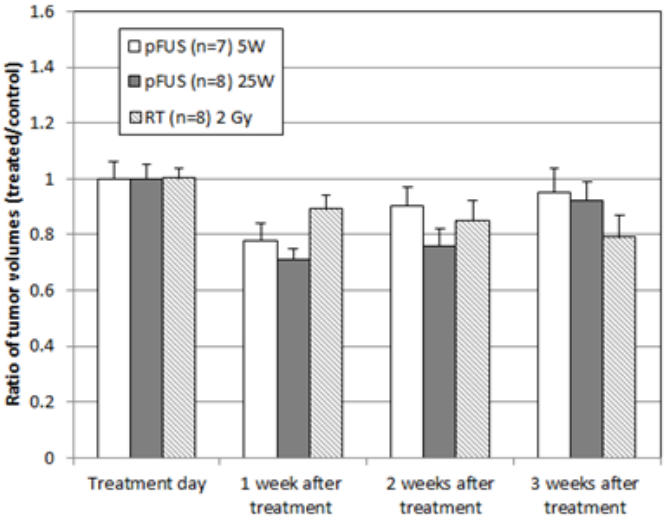

Figure 7: The ratio of the mean tumor volumes for mice implanted with prostate (LNCaP) cancer cells treated by RT (2Gy, n = 8) and pFUS with 1 exposure at 5W and 50% duty cycle (n = 7) and at 25W and 10% duty cycle (n = 8) to the mean tumor volume for the control mice (n = 12) at different times post treatment.

It can be seen that the tumor growth delay in mice treated with pFUS at both 5 W and 25 W power settings indicated an earlier cell death than that in RT treated animals; the most significa t tumor volume difference between the control mice and pFUS treated mice was observed one week after treatment (22% at 5 W and 29% at 25 W) while the most significa t tumor volume difference between the control mice and RT treated mice was observed three weeks after treatment (21% for 2Gy). The pFUS results for the 25 W power setting were taken from our previous investigations [23].

DISCUSSION

In this study, we have investigated the feasibility of pFUS for cancer treatment using a clinical HIFU treatment system with MR image guidance. This was an expansion of our previous *in vivo* experiments to investigate the nonthermal effect of pFUS on cancer cell killing using both in vitro cell survival methods and *in vivo* animals implanted with different tumor cell lines and different pFUS parameter settings. Our *in vitro* results indicated significa t cell killing effects by pFUS exposures at different power settings (6 W and 10 W) and for different tumor cell lines (LNCaP and PC3). Since the temperature elevation within the focal volume was controlled to within 5°C, the cell damage is considered to be predominantly nonthermal. However, since the tumor cells were suspended in tissue culture, additional cell damage from mechanical force (fluid circulation inside the container) could not be ruled out, which will not occur with tumor cells in animals. This would potentially result in an overestimation of the therapeutic effect of pFUS. Since this effect is expected to be more significa t with increased ultrasound intensities, no further experiments were performed at higher acoustic power settings. Therefore, we believe that the in vivo experiments with tumor-bearing mice will be more reliable to quantify the therapeutic effect of pFUS.

In the *in vivo* study, mice were implanted with either prostate or breast tumor cells. Large variations of tumor take-up rates and growth rates were observed between the two cell lines and between different batches of mice. It was found that when the tumors were relatively small, they grew more consistently following an exponential growth. As the tumors grew larger, the variations of the tumor growth rate increased for both control and pFUS or RT treated mice (also depending on the tumor size when the treatment was performed),

leading to greater statistical uncertainties in the mean tumor volume values, especially at later time points post treatment. In order to minimize the statistical uncertainty, a control group was always included in each experiment, which used the same batch of mice, and mice of similar tumor volumes were randomly assigned into different treatment groups and the control group. The same strategy was also used in our previous studies (e.g., [23]).

The cell killing mechanisms of pFUS were investigated in a previous study [23] by immunohistochemical staining of caspase 3 at 24 hours after treatment and γH2AX and Chk2 at 48 hours after treatment. Elevated levels of γH2AX and Chk2 expressions in tumor cells exposed to pFUS indicated the presence of DNA damage, resulting in mitotic cell death or clonogenic cell death. Pulsed FUS also induced apoptotic cell death in tumor cells, which may not be as significa t as mitotic cell death, but one could not preclude the contribution of spontaneous and induced apoptosis in pFUS treated tumors to the early treatment response (i.e., the largest tumor growth delay occurred at one week after treatment).In contrast, the largest tumor growth delay by 2Gy radiation occurred at three weeks after RT treatment (Figure 7). The early response of pFUS treated tumors suggested other mechanisms besides mitosis and apoptosis that might cause cell damage leading to necrosis. Due to the dynamic characteristics of ultrasound, ultrasound induced cavitations undergoes reactions involved in ultrasound physics and ultrasound chemistry, damaging cell membranes and intracellular structures, and ultimately resulting in cellular injury and early cell death [26,27].

In this work, we have used pFUS parameter settings of 5 W with 50% duty cycle and 25W with10% duty cycle for the pFUS sonication, which generated a temperature elevation less than 5°C in our phantom measurements and in targeted tumor tissues in mice as measured by MR thermometry. Both pFUS parameter settings delivered the same acoustic energy for the same sonication duration, leading to a similar temperature elevation. However, the total acoustic energy is not expected to correlate with the nonthermal therapeutic effect of pFUS. To facilitate the clinical application of pFUS, a special dosimetric quantity will be needed to quantify its therapeutic effect and for future experimental design and treatment planning. The 10% duty cycle was the lowest duty cycle available on this clinical HIFU system, and therefore, the 25W acoustic power would provide the highest intensity for our experiments, keeping the total energy input unchanged. The average tumor growth delay with this acoustic power was about a week for LNCaP cells, which was more effective than the power setting of 5 W and 50% duty cycle (Figure 5). For MHC-7 cells, the average tumor growth delay was about two weeks at 25 W and 10% duty cycle (Figure 4). This difference may refle t the differential response of various tumor cells (i.e., MCF-7 and LNCaP) to pFUS and their repopulation rates.

Our preliminary results showed that the therapeutic effect of pFUS could be increased with higher ultrasound intensities, which can be achieved with lower duty cycles, to keep the temperature elevation below 5°C for the same sonication duration (Figure 7). Our preliminary results also demonstrated the possibility of repeated pFUS exposures for additional cell damage. This indicates that we can perform multiple fractionated pFUS treatments. The side-by-side comparison of pFUS and RT results of tumor growth delay provided useful information for the design of future studies on the dose-response relationship and fractionation effects of pFUS for cancer therapy. Conventional RT typically uses 2 Gy as a daily dose. Our pFUS results showed more significa t tumor growth delay than a daily RT treatment. In this work, the temperature in the focal volume has been kept below 42°C to investigate the nonthermal effect of pFUS treatment. This condition should not be a limitation on the potential clinical applications of pFUS. Ideally, nonthermal pFUS may be combined with thermal ablation, hyperthermia and other therapies such as RT and chemotherapy to achieve the best tumor control clinically.

Further experiments are warranted to test various pFUS parameters and different tumor models to provide useful pre-clinical data for clinical trial designs. It should be noted that in this work, the sonication volume was usually larger than the tumor volume, especially in the longitudinal direction (ultrasound beam axis), and; therefore, the surrounding normal structures (e.g., skin, muscles, rectum, bladder, bowel) should have received similar pFUS exposures. Although the pFUS treatment induced considerable cancer cell death, no noticeable normal tissue toxicities were observed either in pFUS treated mice immediately after treatment or in sacrifi ed mice in this work.

CONCLUSIONS

In this work, we have investigated the nonthermal therapeutic effect of pFUS using in vitro cell survival studies and *in vivo* mouse tumors implanted subcutaneously and orthotopically. Our preliminary results show that pFUS has significa t therapeutic potential; the in vitro cell death and in vivo tumor growth delay by one sonication (5 W acoustic power and 50% duty cycle; 25W acoustic power and 10%

DOI: https://doi.org/10.30654/MJCS.10025

duty cycle) was comparable to that of 2Gy radiation for the breast and prostate tumors investigated. There was no tissue damage in normal organs surrounding the prostate cancer implanted orthotopically in sacrifi ed animals or skin damage after the pFUS treatment of the breast cancer implanted subcutaneously. This indicated a favorable therapeutic ratio for repeated pFUS treatment to achieve tumor control. More systematic animal studies are being carried out to derive optimal ultrasound parameters and fractionation schemes to maximize the therapeutic potential of pFUS. Further investigations are warranted to understand the mechanism of pFUS-induced nonthermal cell damage and to develop special equipment for clinical testing of pFUS therapy.

ACKNOWLEDGMENTS

This publication was supported by grant number P30 CA006927 from the National Cancer Institute, NIH. Its contents are solely the responsibility of the authors and do not necessarily represent the officia views of the National Cancer Institute or the National Institutes of Health. We would like to thank the core research facilities at FoxChase Cancer Center for their technical support. This work was supported in part by DOD PC073127, DOD BC102806, Focused Ultrasound Surgery Foundation and Varian Medical Systems.

REFERENCES

1. Cline HE, Schenck JF, Hynynen K, Watkins RD, et al. (1992). MR-Guided Focused Ultrasound Surgery. J Comput Assist Tomogr. 16(6):956-65.
2. Kohrmann KU, Michel MS, Gaa J, Marlinghaus E, et al. (2002). High intensity focused ultrasound as noninvasive therapy for multilocal renal cell carcinoma: Case study and review of the literature. J Urol. 167(6):2397-2403.
3. Tempany CMC, Stewart EA, McDannold N, Quade BJ, et al. (2003). MR imaging-guided focused ultrasound surgery of uterine leiomyomas: A feasibility study. Radiology. 226(3):897-905.
4. Illing RO, Kennedy JE, Wu F, ter Har GR, et al. (2005). The safety and feasibility of extracorporeal high-intensity focused ultrasound (HIFU) for the treatment of liver and kidney tumours in a Western population. Br J Cancer. 93(8):890-895.
5. Wu F, Wang ZB, Zhu H, Chen W, et al. (2005). Feasibility of US-guided high-intensity focused ultrasound treatment in patients with advanced pancreatic cancer: Initial experience. Radiology. 236(3):1034-1040.
6. Stewart EA, Rabinovici J, Tempany CMC, Inbar Y, et al. (2006). Clinical outcomes of focused ultrasound surgery for the treatment of uterine fib oids. Fertil Steril. 85(1):22-29.
7. Ter Haar G, Coussios C. (2007). High intensity focused ultrasound: past, present and future. Int J Hyperthermia. 23:85-87.
8. Chu KF, Dupuy DE. (2014). Thermal ablation of tumours: Biological mechanisms and advances in therapy. Nat Rev Cancer. 14, 199–208.
9. Bednarski MD, Lee JW, Callstrom MR, Li KC. (1997). In vivo target-specific delivery of macromolecular agents with MR-guided focused ultrasound. Radiology. 204(1):263-268.
10. Nelson JL, Roeder BL, Carmen JC, Roloff F. (2002). Ultrasonically activated chemotherapeutic drug delivery in a rat model. Cancer Res. 62(24):7280-7283.
11. Dittmar KM, Xie JW, Hunter F, Trimble C, et al. (2005). Pulsed high-intensity focused ultrasound enhances systemic administration of naked DNA in squamous cell carcinoma model: Initial experience. Radiology. 235(2):541-546.
12. Yuh EL, Shulman SG, Mehta SA, Xie J, et al. (2005). Delivery of systemic chemotherapeutic agent to tumors by using focused ultrasound: Study in a murine model. Radiology. 234(2):431-437.
13. Hancock HA, Smith LH, Cuesta J, Durrani AK. et al. (2009). Investigations into Pulsed High-Intensity Focused Ultrasound-Enhanced Delivery: Preliminary Evidence for a Novel Mechanism. Ultrasound Med Biol. 35(10):1722-1736.
14. Chen L, Mu ZM, Hachem P, et al. (2010). MR-guided focused ultrasound: enhancement of intratumoral uptake of H-3 -docetaxel in vivo. Phys Med Biol. 55:7399-7410.
15. Mu ZM, Ma CM, Chen XM, Cvetkovi D, et al. (2012). MR-guided pulsed high intensity focused ultrasound enhancement of docetaxel combined with radiotherapy for prostate cancer treatment. Phys Med Biol. 57(2):535-545.
16. Chen XM, Cvetkovic D, Ma CM, Chen L. (2012). Quantitative study of focused ultrasound enhanced doxorubicin delivery to prostate tumor in vivo with MRI guidance. Med Phys. 39(5):2780-2786.
17. Ma CM, Chen L, Freedman G, Bleicher R. (2009). MR guided Focused ultrasound for high risk and recurrent breast cancer. IFMBE Proceedings WC 2009. 25/VI:140-43.
18. Zhang T, Chen L, Zhang S, Xu Y, et al. (2017). Effects of high-intensity focused ultrasound oncisplatin-resistant human lung adenocarcinoma in vitro and in vivo. Acta Biochim Biophys Sin. 49:1092–1098.

19. Miller DL, Thomas RM, Buschbom RL. (1995). Comet assay reveals DNA strand breaks induced by ultrasonic cavitation in vitro. Ultrasound in medicine & biology. 21(6):841-8.
20. Dalecki D. (2004). Mechanical bioeffects of ultrasound. Annu Rev Biomed Eng. 6:229-48.
21. Feril LB, Kondo T, Cui ZG, Tabuchi Y, et al. (2005). Apoptosis induced by the sonomechanical effects of low intensity pulsed ultrasound in a human leukemia cell line. Cancer letters. 221(2):145-52.
22. Jernberg A. (2007). Ultrasound, ions and combined modalities for increased local tumor cell death in radiation therapy, Ph.D. Thesis. Karolinska Institute, Stockholm, Sweden.
23. Ma CM, Chen XM, Cvetkovic D, Chen L. (2014). An In-Vivo Investigation of the Therapeutic Effect of Pulsed Focused Ultrasound on Tumor Growth. Med Phys. 41,122901. doi: 10.1118/1.4901352.
24. Chen L, Ma CM. (2018). Dosimetry for high-intensity ultrasound treatment, in Recent Advancements and Applications in Dosimetry, Ed. MF Chan (Nova Medical and Health, New York) pp. 1-24.
25. Wang B, Ren JH, Zhang P, Cvetkovic D, et al. (2019). An In-Vivo Study on Pulsed Low-Dose-Rate Radiotherapy for Prostate Cancer. Mathews J Cancer Sci. 4(2): 21, DOI: https://doi.org/10.30654/MJCS.10021.
26. Zachary JF, Blue JP, Miller RJ, O'Brien WD Jr. (2006). Vascular lesions and sthrombomodulin concentrations from auricular arteries of rabbits infused with microbubble contrast agent and exposed to pulsed ultrasound. Ultrasound Med Biol. 32:1781-1791.
27. Miller D, Smith N, Bailey M, Czarnota G, et al. (2012). Overview of Therapeutic Ultrasound Applications and Safety Considerations. J Ultrasound Med. 31(4):623–634.

DOI: https://doi.org/10.30654/MJCS.10025